Extent and feature of lattice distortions around Ga impurity atoms in InSb single crystal

S. Hosokawa,[1,*] N. Happo,[2] T. Ozaki,[3] H. Ikemoto,[4] T. Shishido,[5] and K. Hayashi[5]

[1]*Department of Physics, Graduate School of Science and Technology, Kumamoto University, Kumamoto 860-8555, Japan*
[2]*Graduate School of Information Sciences, Hiroshima City University, Hiroshima 731-3194, Japan*
[3]*Research Center for Condensed Matter Physics, Hiroshima Institute of Technology, Hiroshima 731-5193, Japan*
[4]*Department of Physics, Faculty of Science, University of Toyama, Toyama 930-8555, Japan*
[5]*Institute for Materials Research, Tohoku University, Sendai 980-8577, Japan*

To clarify lattice distortions induced by adding Ga atoms in the InSb crystal, Ga $K\alpha$ x-ray fluorescence holography (XFH) experiments were carried out on an $In_{0.995}Ga_{0.005}Sb$ diluted mixed single crystal, and three-dimensional atomic images around the Ga atoms were reconstructed. Although the atomic images are located almost at ideal positions of the InSb crystal, some differences can be observed for only the first- and second-neighboring atoms. By combining them with x-ray absorption fine structure data, large spatial fluctuations of the first-neighboring atoms appear in the angular direction, which can be clarified from the present XFH results. From the XFH results, it is concluded that lattice distortions are limited within the second neighbors in this diluted mixed crystal, in contrast to five chemical bonds in a heavily doped mixed crystal of $Zn_{0.4}Mn_{0.6}Te$ reported previously.

PACS number(s): 61.72.Dd, 61.72.S−, 61.72.uj

I. INTRODUCTION

$In_{1-x}Ga_xSb$ mixed crystals are widely used for infrared telecommunications as raw materials of detecting and emitting devices, since the narrow band gap of these alloys can be easily controlled by varying x. Due to the large difference between the lattice constants of InSb (0.6479 nm) and GaSb (0.6095 nm) crystals, however, it is difficult to grow $In_{1-x}Ga_xSb$ single crystals except at very low concentrations of Ga or In.

As described in Ref. 1, different and inconsistent results of the nearest neighbor distance r_1 were reported between x-ray diffraction (XD) and x-ray absorption fine structure (XAFS) measurements in many mixed crystals, such as $Si_{1-x}Ge_x$,[2] $Ga_{1-x}In_xAs$,[3–6] $In_{1-x}Ga_xSb$,[7] $ZnSe_{1-x}Te_x$,[8,9] $Cd_{1-x}Zn_xTe$,[10] $Zn_{1-x}Mn_xTe$,[11] $Cd_{1-x}Mn_xTe$,[12,13] and ionic solid solutions.[14,15]

For example, Fig. 1 shows the x dependence of r_1 for $In_{1-x}Ga_xSb$ mixed crystals,[7] being taken up in this paper. From the lattice constant a obtained from XD showing sharp Bragg peaks even for mixtures, the bond lengths were calculated for their zinc-blende structure, $\sqrt{3}a/4$, which are given by triangles in Fig. 1. As clearly seen in the figure, the XD results show Vegard's law[16] behavior, i.e., they linearly change with x. On the contrary, results from the XAFS experiments given by the circles indicate that r_1 changes very little with x; it looks largely keeping Pauling's bond length[17] of Ga-Sb and In-Sb, different largely by about 0.018 nm.

This serious discrepancy arises from the different length scales investigated by XD and XAFS. The XD technique can, in principle, detect the *periodicity* of a perfect single crystal. The powder diffraction method is also a powerful tool for determining the crystal system and its lattice constants for polycrystalline materials. If the sample is not a perfect crystal, e.g., modified by mixing other elements, however, XD cannot determine the positions of the constituent elements perfectly, because the perfect periodicity of the atomic structure is broken, conferring randomness in atomic positions. Thus,

one should recognize that XD is not ideal for investigating structures of nonperfect crystals, e.g., mixed crystals, and that this method is very *farsighted*.

On the other hand, XAFS is widely used for investigating *local* atomic structures around a specific element, and can be adopted even for disordered materials. With this method, however, one can obtain only one-dimensional information, i.e., directionally averaged pair distribution functions. Moreover, detectable information is usually limited to the second- or third-neighboring atoms due to the short mean-free path length of x-ray excited photoelectrons. In this sense, the XAFS technique is very *nearsighted*.

To bridge the two techniques with very different length scales, an experimental attempt was carried out by Petkov *et al.*[5] on $Ga_{1-x}In_xAs$ mixed crystals. Nearest- and further-neighbor distances as well as bond length distributions were obtained from high real-space resolution atomic pair distribution functions (PDFs) by high-energy XD measurement. In these PDFs, the first peak is clearly resolved into two subpeaks corresponding to the Ga-As and In-As bond lengths, which are in good agreement with the XAFS results.[3,4] Moreover, the PDFs show that a higher neighbor structure exhibits Vegard's law-type behavior beyond ~1 nm. Alternative attempts were also made by extending the experimental survey range of XAFS to longer distances.[9,15]

A plausible model was proposed by Mikkelsen and Boyce[4] for $Ga_{0.5}In_{0.5}As$, which is an analogy of a chalcopyrite crystal. Another model was the extension of this model to the entire concentration range by Barzarotti *et al.*[12,13] for $Cd_{1-x}Mn_xTe$ diluted magnetic semiconductors with the same zinc-blende crystal structure. Both models were based on the idea that Vegard's law was preserved in one of the sublattices and that Pauling's lengths were realized by shifting atoms on another sublattice. From these experiments and these models, however, it is very difficult to determine where Pauling's bond length interconnects with Vegard's law, or where the local lattice distortions vanish.
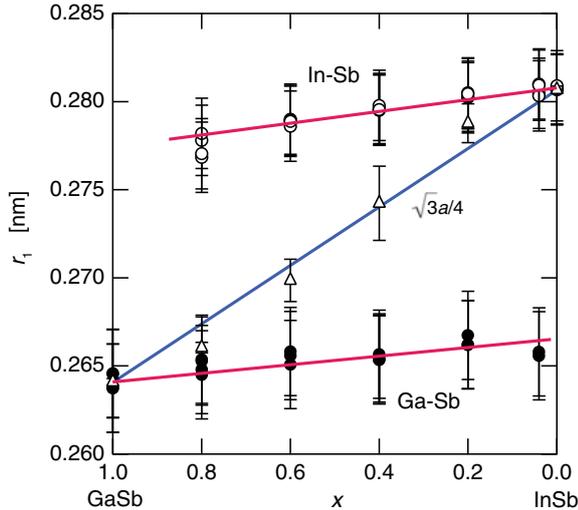
FIG. 1. (Color online) Concentration dependence of nearest neighbor distances obtained from XD (triangles) and XAFS (circles) measurements of $In_{1-x}Ga_xSb$ mixed crystals. The lines are the guides for eyes. The figure is taken from Ref. 7.

To make an appropriate connection between *farsighted* XD and *nearsighted* XAFS results, a new experiment is necessary to investigate the intermediate-range order in mixed crystals. For this, x-ray fluorescence holography (XFH) developed by Tegze and Faigel[18] and Tegze *et al.*[19] is a good and reliable method for the structure characterization of crystals.

XFH enables one to obtain three-dimensional (3D) images. This can explicitly determine the position of neighboring atoms with respect to a specific element emitting fluorescent x rays without the use of a special atomic model. We have adopted this technique for a heavily doped mixed single crystal of $Zn_{0.4}Mn_{0.6}Te$ by measuring Zn $K\alpha$ XFH to clarify how Pauling's bond length picture reconciles with Vegard's law by observing the image intensities of the surrounding atoms with different lengths from the central Zn atoms.[1] We found that Pauling's scheme interconnects with Vegard's law at about five chemical bonds, and that the randomness of atomic positions is well explained by our original model named the *locomotive wheel* atomic configuration model.

In this paper, we will show the feasibility of XFH for investigating the lattice distortions of $In_{1-x}Ga_xSb$ mixed crystals with a low content of $x = 0.005$ together with an undoped GaSb crystal by performing Ga $K\alpha$ XFH. Interest is focused on whether the single-crystal growth ability depends on the extent of lattice distortions by comparing the results with those of a heavily doped $Zn_{0.4}Mn_{0.6}Te$.

II. EXPERIMENTAL PROCEDURE

$In_{0.995}Ga_{0.005}Sb$ and GaSb single crystal samples were grown at the Advanced Research Center of Metallic Glasses, Institute for Materials Research, Tohoku University, using a Czochralski method. The crystals were cut and polished so as to have (111) flat surfaces larger than 5×5 mm^2. The crystallinity of the samples was examined by taking Laue photographs.

XFH measurements were carried out at the beamlines BL6C and BL15B1 in the Photon Factory at the High Energy Accelerator Research Organization (PF-KEK) in Tsukuba, Japan. The samples were placed on a two-axes table of a diffractometer. The measurements were performed in inverse mode by rotating the two axes, the exit angle of $0° \leqslant \theta \leqslant 70°$ in steps of $1°$, and the azimuthal angle of $0° \leqslant \phi \leqslant 360°$ in steps of about $0.35°$, of the sample stage. Incident x rays were focused onto the (111) surface of the samples. Ga $K\alpha$ fluorescent x rays were collected using an avalanche photodiode detector with a cylindrical graphite crystal energy analyzer. The XFH signals were recorded at eight different incident x-ray energies from 10.5 to 14.0 keV in steps of 0.5 keV. Each scan took about 11 h. Details of the experimental setup are given elsewhere.[20–22]

Hologram oscillation data were obtained by subtracting the background from the normalized intensities. An extension of the hologram data was carried out to the perfect 4π sphere using the crystal symmetry of the cubic zinc-blende structure and the measured x-ray standing wave (XSW) lines. Since a Fourier transform of the XFH data with a single incident energy produces false twin images,[22,23] a 3D atomic image was reconstructed using Barton's algorithm[24] by superimposing the holograms with eight different incident x-ray energies, which can highly suppress the appearance of twin images.

For comparison to the experimental data, theoretical holograms were calculated using model clusters, one taken from the GaSb crystal structure (GaSb cluster model) and another taken from the InSb crystal but with the central In atom replaced by a Ga atom (undistorted InGaSb cluster model). The former is a model for the GaSb XFH data, and the latter for the $In_{0.995}Ga_{0.005}Sb$ XFH data. Detailed calculation procedures are given elsewhere.[25] The calculation was performed on the assumption of the random distributions of ions around lattice centers. The lattice constants were fixed to the original crystal values of 0.6095 nm for the GaSb cluster model and 0.6479 nm for the undistorted InGaSb cluster model. The cluster radius was about 6 nm, which contains about 35 000 atoms around the central Ga atom. The atomic scattering intensities from the neighboring atoms were obtained using literature data of atomic form factors,[26] Debye-Waller factors,[27] and absorption coefficients.[28]

III. RESULTS

Figure 2 shows examples of the Ga $K\alpha$ hologram patterns of (a) $In_{0.995}Ga_{0.005}Sb$ and (b) GaSb single crystals measured at an incident x-ray energy of 11.0 keV. The radial and angle directions indicate θ and ϕ, respectively, and the magnitudes are given as the color bars beside the figures. Clear threefold symmetry images including strong XSW signals were observed in the patterns indicating the good qualities of the single crystals. Note that the magnitude of modulation is weaker in GaSb than in $In_{0.995}Ga_{0.005}Sb$ due mainly to the x-ray scattering cross section of Ga being much smaller than that of In.

Figures 3(a) and 3(b) show the reconstructed atomic images of $In_{0.995}Ga_{0.005}Sb$ and GaSb single crystals, respectively, on the (110) plane around the central Ga atoms marked by crosses. Circles in (a) and (b) indicate the ideal atomic positions of InSb and GaSb crystals, respectively. The image intensities were

(a) $In_{0.995}Ga_{0.005}Sb$
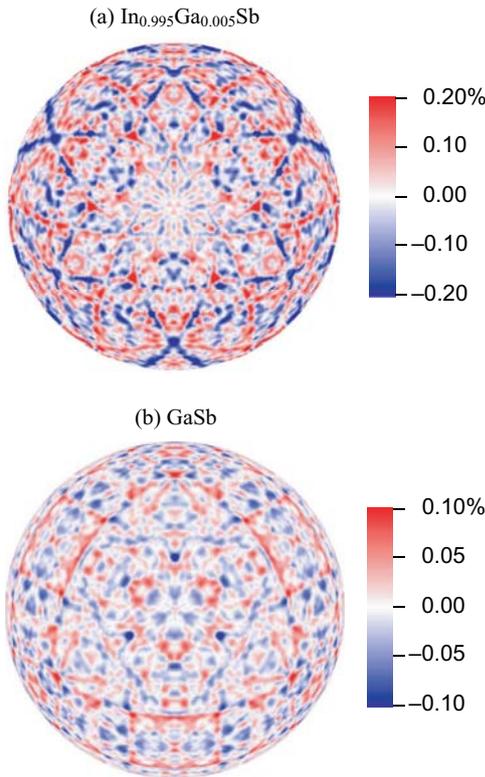
(b) GaSb

FIG. 2. (Color online) Examples of the Ga $K\alpha$ hologram pattern obtained from (111) surfaces of (a) $In_{0.995}Ga_{0.005}Sb$ and (b) GaSb single crystals measured at an incident x-ray energy of 11.0 keV.

normalized to that of the first-neighboring Sb atoms in the GaSb crystal, and are shown as color bars beside the figures. To avoid confusion on the noise-level artifacts and to emphasize the middle intensity range, the color variation was chosen to range from 0.25 to 0.75.

The origin of artifacts is twin images,[22,23] limited k range, experimental noises, and extinction effect. The long spatial range periodicity in single crystals induces the XSW lines in holograms.[29–32]. Korecki *et al.*[32] pointed out large influences of the extinction effect on the holographic signals, i.e., this effect produces sharp symmetric lines lying on the XSW lines in holograms, resulting in artifacts in real-space atomic images. In fact, clear modifications of the XSW lines seem to be observed in the present holograms shown in Fig. 2. Note that as pointed out also by Korecki *et al.*,[32] such extinction-induced artifacts can be suppressed by multiple energy algorithms[19,24] as in the present study. An improvement of statistical quality of experimentally obtained holograms is also important to reduce artifacts as discussed at the end of this section.

As a guide for eyes, the (110) plane in a zinc-blende crystal of $In_{0.995}Ga_{0.005}Sb$ is schematically illustrated in Fig. 3(c). The small circles indicate the cation (In or Ga) atoms occupying the even-neighboring sites, and the large circles indicate the anion Sb atoms located at odd-neighboring sites. The thick circles are located on the (110) plane, and correspond to the atomic images in Figs. 3(a) and 3(b).

Figures 4(a) and 4(b) show the reconstructed atomic images of $In_{0.995}Ga_{0.005}Sb$ and GaSb single crystals, respectively, on the (004) plane around the central Ga atoms located below the

(a) $In_{0.995}Ga_{0.005}Sb$

(b) GaSb

(c)
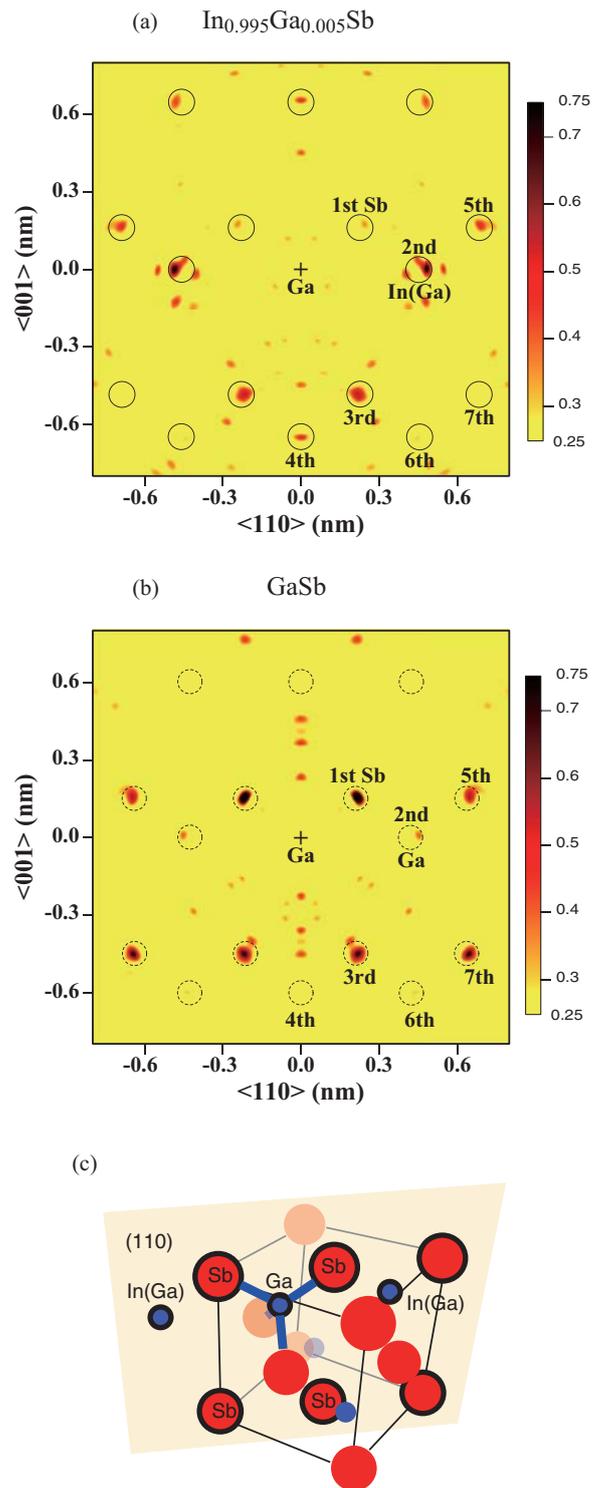
FIG. 3. (Color online) Atomic images of (a) $In_{0.995}Ga_{0.005}Sb$ and (b) GaSb on the (110) plane around the central Ga atoms marked by crosses. Circles indicate the ideal atomic positions of the corresponding (a) InSb and (b) GaSb. (c) Schematic view of the zinc-blende structure of a $In_{0.995}Ga_{0.005}Sb$ mixed crystal. Small circles indicate In or Ga atoms, and large circles indicate Sb atoms. Thick circles are located on the (110) plane, corresponding to the atomic images in (a) and (b).

center of the figures by $a/4$, where a is the lattice constant of the fcc structure. Circles in (a) and (b) indicate the ideal

(a) $In_{0.995}Ga_{0.005}Sb$

(b) GaSb

(c)
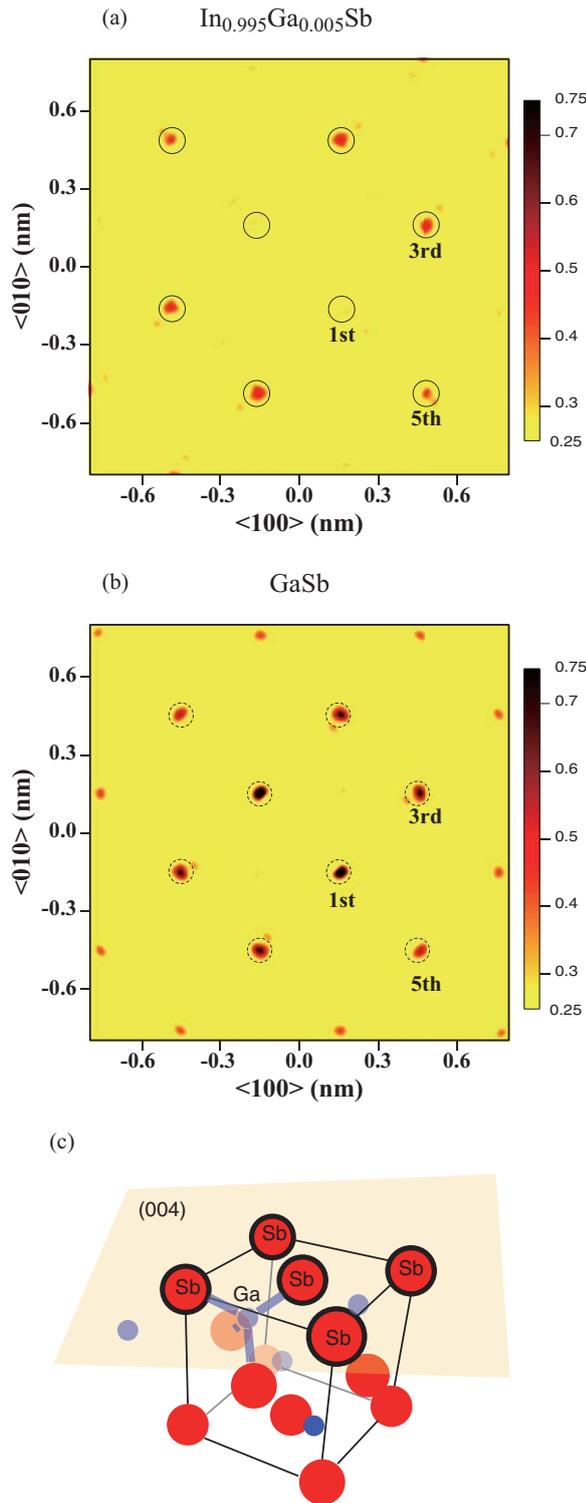
FIG. 4. (Color online) Atomic images of (a) $In_{0.995}Ga_{0.005}Sb$ and (b) GaSb on the (004) plane. Circles indicate the ideal atomic positions of the corresponding (a) InSb and (b) GaSb. (c) Schematic view of the zinc-blende structure of an $In_{0.995}Ga_{0.005}Sb$ mixed crystal. Small circles indicate In or Ga atoms, and large circles indicate Sb atoms. Thick circles are located on the (004) plane, corresponding to the atomic images in (a) and (b).

atomic positions of InSb and GaSb crystals, respectively. As a guide for eyes, a zinc-blende crystal of $In_{0.995}Ga_{0.005}Sb$ is

schematically illustrated in Fig. 4(c). The small circles indicate the cation (In or Ga) atoms, and the large circles indicate the anion Sb atoms. The thick circles are located on the (004) plane, and correspond to the atomic images in Figs. 4(a) and 4(b).

As expected from the XD data, the positions of the atomic images in $In_{0.995}Ga_{0.005}Sb$ are located near those of the InSb crystal, reasonable for a mixed crystal with a diluted Ga concentration. The image intensities of the first-neighboring atoms in the $In_{0.995}Ga_{0.005}Sb$ crystal shown in Figs. 3(a) and 4(a) are, however, extremely weaker than those in the GaSb crystal shown in Figs. 3(b) and 4(b), respectively. In addition, the features of the second-neighboring cation (In or Ga) atoms in $In_{0.995}Ga_{0.005}Sb$ shown in Fig. 3(a) are very complex, and some artifacts are still located around the ideal positions. We suppose that most of the second-neighboring In(Ga) atoms are located at the ideal positions, while some of them are shifted due to the lattice distortions by the central Ga impurity atom. On the other hand, the intensities of the second-neighboring Ga atoms in GaSb shown in Fig. 3(b) are weak but single, which is only due to the small x-ray scattering cross section of Ga compared to those of In and Sb. On the contrary, the image intensities of distant Sb atoms beyond the third-neighboring Sb atoms seem to be comparable between the $In_{0.995}Ga_{0.005}Sb$ and GaSb crystals, as shown in Figs. 4(a) and 4(b), respectively.

Preliminary results of the atomic images of the $In_{0.995}Ga_{0.005}Sb$ diluted mixed crystal were reported in our previous paper.[7] Due to the increase in the number of imposed holograms from five to eight different incident energies, however, the quality of the reconstructed images is highly improved. Moreover, the data of the GaSb crystal were also achieved under the same experimental conditions, which enables us to use them for further discussion.

Here, we should mention how the present XFH data improved in detail by comparing them to those in our previous paper.[7] The three additional XFH data sets were taken at BL15B1 of the PF-KEK, where the flux of the incident x rays is much stronger than that of BL6C by more than one order of magnitude in the high energy region. With this advantage, the effects of adding three XFH data sets were threefold: (1) the statistical quality was highly improved; (2) due to the short wavelength, the resolution of the images improved; (3) the twin artifacts were reduced and the real images were enhanced as explained above. For example, many of the artifacts shown in Figs. 3 and 5 in our previous paper[7] were highly suppressed. In particular, the most important result was realized, i.e., stronger images of the first-neighboring Sb atoms located at a larger distance in Fig. 3 of Ref. 7 are highly suppressed and mostly invisible in Fig. 3(a), while weaker ones at a shorter distance remain unchanged. Thus, it can be concluded that the former images are artifacts and the latter ones are real.

IV. DISCUSSION

Since the quality of the images was highly improved from that in our previous report,[7] quantitative analyses of the fluctuations in the atomic positions of individual neighboring atoms became possible, since the image intensities are highly
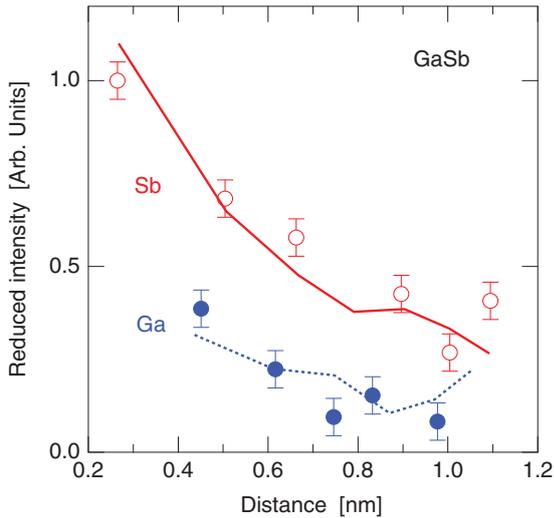
FIG. 5. (Color online) Experimental image intensities of the Sb (empty circles) and Ga (full circles) atoms in the GaSb crystal as a function of the distance from the central Ga atom. The theoretical intensities of the Sb and Ga atoms using the GaSb cluster model are given by solid and dotted curves, respectively.

related to positional fluctuations, which can be precisely estimated by comparing them to the theory.[1,22,33]

For a start, the validity of the cluster theory was examined using the GaSb crystal data. The empty and full circles in Fig. 5 indicate the image intensities of the Sb and Ga atoms obtained from the XFH experiment, respectively, as a function of the distance from the central Ga atom. The solid and dotted curves represent the theoretical results for the Sb and Ga atoms, respectively, using the GaSb cluster model. These intensities are reduced so that the theoretical Sb data fit well to the experimental values of the first- and third-neighboring Sb atoms. The scaling factor of the experimental and theoretical intensities is 0.070. This remarkable reduction of the experimental intensity originated from mainly the directional dependence of the absorption for incident x rays

in crystals.[32] Comparisons of theory and experiment on this effect were performed in several papers.[32,34]

Although the experimental data are rather scattered, particularly in the low intensity region, the theory reproduces the tendency of the experimental results in the intensities of both the Sb and Ga atoms. Thus, the theoretical results can be reliably used as a reference for the $In_{0.995}Ga_{0.005}Sb$ diluted mixed crystal.

The empty circles in Fig. 6(a) show the experimentally obtained image intensities of the Sb atoms in the $In_{0.995}Ga_{0.005}Sb$ crystal. The vertical scale is the same as that in Fig. 5. The solid curve indicates the theoretical results of the Sb atoms using the undistorted InGaSb cluster model. The scaling factor of the experimental and theoretical intensities is 0.187. As clearly seen in the figure and mentioned in the last section, the image intensities of the first-neighboring Sb atoms in the $In_{0.995}Ga_{0.005}Sb$ crystal are very weak with respect to those of the theoretical reference value. On the other hand, the intensity of the third-neighboring Sb atoms mostly recovers to the theoretical reference value. The ratios of these experimental and theoretical values are 0.35 and 0.89 for the first- and third-neighboring Sb atoms, respectively, as given below the marks in Fig. 6(a).

Full circles in Fig. 6(b) show the experimentally obtained image intensities of the cation atoms (mostly In atoms) in the $In_{0.995}Ga_{0.005}Sb$ crystal. The dotted curve represents the theoretical results of the In atoms using the undistorted InGaSb cluster model. As seen in the figure, the experimental results of cation image intensities are in good agreement with those obtained from the undistorted InGaSb cluster model. Thus, it is concluded that, concerning the XFH image intensities, only the first-neighboring Sb atoms in the $In_{0.995}Ga_{0.005}Sb$ crystal are contradictory to the theoretical calculations. Note that this result is different from the previous finding in a heavily doped mixed crystal of $Zn_{0.4}Mn_{0.6}Te$,[1] where the weaknesses of the atomic images were observed for more distant atoms with five chemical bonds from the dopant atom.

To understand the observation of the weak intensities of the first-neighboring Sb atoms, we introduce an atomic model
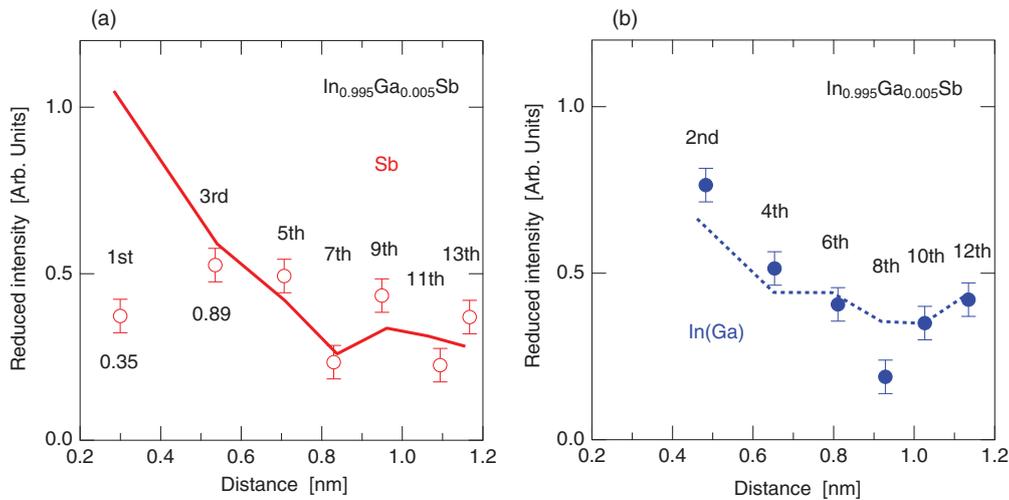
FIG. 6. (Color online) Experimental image intensities of the (a) Sb (empty circles) and (b) In(Ga) (full circles) atoms in the $In_{0.995}Ga_{0.005}Sb$ crystal as a function of the distance from the central Ga atom. The theoretical intensities of the (a) Sb and (b) In atoms using the undistorted InGaSb cluster model are given by the solid and dotted curves, respectively.
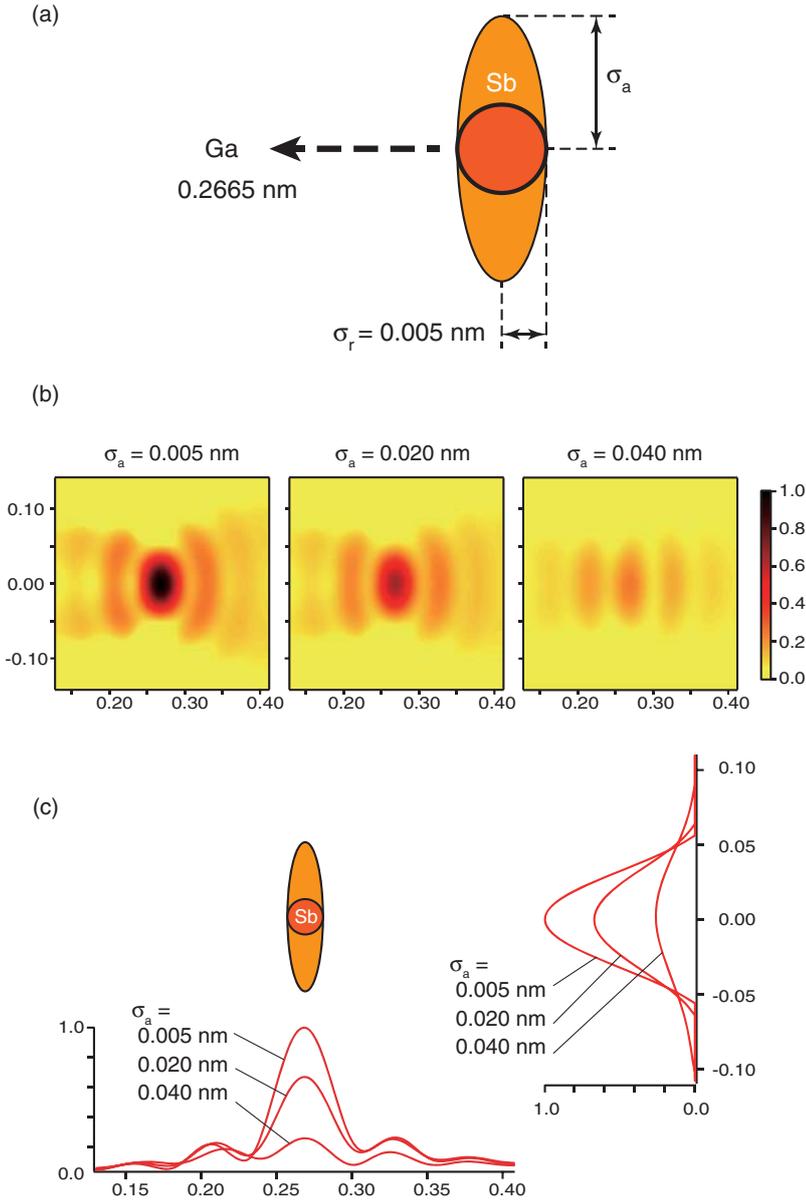
FIG. 7. (Color online) (a) Schematic view of disk model. (b) Atomic images at different σ_a values. (c) Image intensities with varying σ_a.

with positional fluctuations. Since the spatial resolution of the XFH images is about 0.05 nm,[35] the atomic distributions within 0.05 nm are not well resolved by this method. However, such spatial atomic fluctuations largely affect the XFH image intensity.[1,22,33]

Further theoretical calculations of the image intensity were performed with help of the XAFS data. The average length of the Ga-Sb bonds was fixed at 0.2665 nm, which was estimated from the extrapolation of the XAFS data shown in Fig. 1.[7] The XAFS data also provide the mean-square displacement along the radial direction, σ_r, which was estimated to be 0.005 nm. Then, σ_r was fixed, and only the mean-square displacement along the angular direction, σ_a, was varied. For simplicity, the angular direction was approximated to be perpendicular to the radial direction, as shown in Fig. 7(a), and a disklike atomic distribution was used for the theoretical calculations.

Figure 7(b) shows the atomic images obtained at different σ_a values ranging from 0.005 to 0.040 nm. The directions of the images are the same as those for the model shown

in (a). With increasing σ_a, the intensity of the images of the first-neighboring Sb atom decreases gradually. However, the feature of the images does not change systematically, i.e., although the atomic distribution of the model becomes disklike with increasing σ_a, the calculated image does not change in shape, largely keeping a basic oval shape. This result is also confirmed in Fig. 7(c), where the calculated image intensities are plotted over the radial and angular directions from the Sb lattice center. With increasing σ_a, the calculated image shows only a slight broadening with a systematic decrease in the peak height. This is due to the relatively poor spatial resolution of the XFH ($\sim$0.05 nm). Note that the spatial resolution is not isotropic, i.e., the width of the image along the radial direction is about 30% better than that along the angular direction although artifacts are seen in this direction. [See the result at $\sigma_a = 0.005$ nm $= \sigma_r$ in Fig. 7(c).]

Figure 8 shows the σ_a dependence of the calculated image intensity of the first-neighboring Sb atoms. The resultant intensities were normalized to the undistorted value at $\sigma_a =$
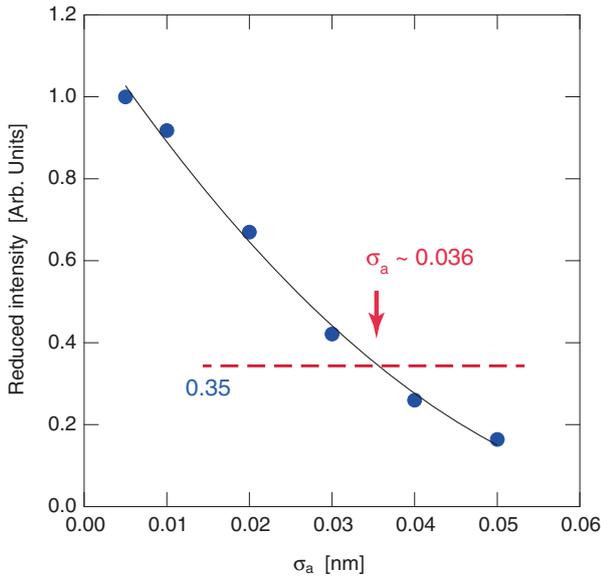
FIG. 8. (Color online) σ_a dependence of the calculated image intensity of first-neighboring Sb atoms.

FIG. 9. (Color online) Schematic views of (a) InSb and (b) that with a Ga dopant obtained from the present XFH result. Arrows indicate the atomic shifts induced by adding a Ga dopant.

$\sigma_r = 0.005$ nm. As a result, $\sigma_a = 0.036$ nm was obtained to reproduce the XFH image intensities of the first-neighboring Sb atoms of 0.35 in the $In_{0.995}Ga_{0.005}Sb$ crystal, which is twice as large as the difference between the Ga-Sb and In-Sb bond lengths, i.e., 0.018 nm.

As regards the second neighbors, they are mainly (99.5%) In atoms, and thus, clear atomic images should appear if they do not have large positional uncertainties. As shown in Fig. 3(a), the main images of the second-neighboring cations were clearly observed, and the image intensity mostly coincides with the theoretical calculation, as shown in Fig. 6(b). However, some distinct artifacts are seen around the ideal positions. These features were not observed in the second-neighbor images in the $Zn_{0.4}Mn_{0.6}Te$ crystal.[1] Therefore, the second-neighboring cations are mostly located at the InSb lattice center, but some of them are expected to move from there, which cannot be discussed further at present.

In contrast to the first- and second-neighboring atoms, the image intensities of the third- and more-distant-neighboring atoms in the crystal are almost the same as those of the theoretical calculations using the undistorted InGaSb model, indicating that the lattice distortions by the Ga dopant vanish beyond the third neighbors from the Ga impurity atom, which results in the data of the XD experiment shown in Fig. 1.[7]

Figure 9 shows schematic views of (a) the InSb lattice and (b) that with a Ga dopant obtained from the present XFH result. The sizes and directions of the ovals indicate the magnitudes of the spatial fluctuations of the constituent atoms, and arrows represent the lattice distortions induced by adding the Ga dopant. The present XFH results revealed that the lattice distortions of the InSb crystal induced by the Ga impurities occur within the second neighbors, and the periodicity of the $In_{0.995}Ga_{0.005}Sb$ mixed crystal is formed by distant atoms with atomic lengths larger than third neighbors.

Note that the vanishment of the lattice distortions occurs at only *three* chemical bonds in the present $In_{0.995}Ga_{0.005}Sb$ diluted mixed crystal, whereas the recovery to Vegard's law
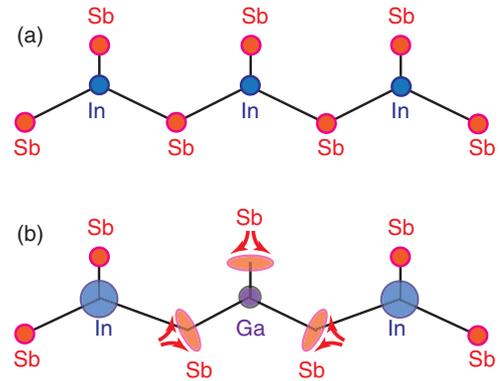
occurs at *five* chemical bonds in the $Zn_{0.4}Mn_{0.6}Te$ heavily doped mixed crystal.[1] At present, it is not clear whether this difference comes from only the concentration of the dopant or the difference in flexibility in the tetrahedral configurations in the mixed crystals. The latter may be related to the difference in the concentration ranges where the single crystals can be formed.

Note that such local lattice distortions in individual neighboring atoms can only be clarified from the XFH data. For example, Wei *et al.*[36] investigated local structures around some impurity atoms, with larger atomic radii, in a Si crystal by a detailed XAFS measurement. From the results, they proposed the model shown in Fig. 8 of Ref. 36, where the dopant atom pushes the first-neighboring Si atom in the radial direction. However, further information on lattice distortions is still lacking because the structural information from the XAFS measurement is limited to be one-dimensional, and mostly up to the second-neighboring atoms. In contrast, Hayashi *et al.*[37] discussed the distortions of the second- and further-distant-neighboring atoms around the Ge impurity by XFH.

Existing models discussing atomic arrangements in mixed crystals were introduced in our previous paper,[1] such as Mikkelsen-Boyce's chalcopyrite analogy[4] and Barzarotti's sublattice distortion model.[12,13] In contrast to these models, the present XFH results revealed that lattice distortions may occur in both of the sublattices, and in the limited spatial range from the dopant. It can be mentioned that the above models insisted too strictly on trying to reproduce the XD results on the entire length scale. On the other hand, the Bragg peaks of the XD data appear, in principle, if the average position of each atom roughly form a periodic condition.

Based on the above scheme, a model was used in our previous paper[1] named the *locomotive wheel* model, which was adopted successfully for the analysis of the XFH data of a heavily doped $Zn_{0.40}Mn_{0.6}Te$ crystal. In this model, each atom is always located on a sphere with a certain distance from the average position, d_{dis}, and fluctuates from the sphere with a proper mean-square displacement. The former and latter displacements correspond to the mixed and thermal effects, respectively. The universal d_{dis} was calculated using the model. Using this value, the XD and XAFS data were successfully reproduced even in detailed features of all the existing experimental data of XD and XAFS, as well as mostly

XFH, for the $Zn_{0.4}Mn_{0.6}Te$ crystal. If we try to apply this model to the present diluted mixed crystal, however, the universal d_{dis} should be zero due to the low concentration of the dopant Ga, which forces the return to a perfect crystal. Thus, this model is not suitable for the diluted impurity systems, and an alternative model is necessary for diluted mixed crystals.

V. SUMMARY

Ga $K\alpha$ XFH experiments were performed on an $In_{0.995}Ga_{0.005}Sb$ diluted mixed crystal, and 3D atomic images around the Ga atoms were reconstructed. The atomic images are located almost at ideal positions of the InSb crystal. Compared to the reference theoretical calculation, however, a very weak image intensity was observed for the first-neighboring Sb atoms. The angular positional fluctuations of the first-neighboring Sb atoms were calculated with the help of XAFS data, and an angular fluctuation of 0.036 nm was obtained in the first-neighboring Sb atoms. The atomic images of the second-neighboring cation atoms are not simple, and may have artifacts due to the positional fluctuations of the atoms. From the present XFH results, it is concluded that lattice distortions are limited within second neighbors in this diluted mixed crystal, in contrast to the five chemical bonds in a heavily doped mixed crystal of $Zn_{0.4}Mn_{0.6}Te$ reported previously.

*Corresponding author: hosokawa@sci.kumamoto-u.ac.jp

[1] S. Hosokawa, N. Happo, and K. Hayashi, Phys. Rev. B **80**, 134123 (2009).

[2] I. Yonenaga and M. Sakurai, Phys. Rev. B **64**, 113206 (2001).

[3] J. C. Mikkelsen, Jr., and J. B. Boyce, Phys. Rev. Lett. **49**, 1412 (1982).

[4] J. C. Mikkelsen, Jr., and J. B. Boyce, Phys. Rev. B **28**, 7130 (1983).

[5] V. Petkov, I.-K. Jeong, J. S. Chung, M. F. Thorpe, S. Kycia, and S. J. L. Billinge, Phys. Rev. Lett. **83**, 4089 (1999).

[6] I.-K. Jeong, F. Mohiuddin-Jacobs, V. Petkov, S. J. L. Billinge, and S. Kycia, Phys. Rev. B **63**, 205202 (2001).

[7] S. Hosokawa, T. Ozaki, N. Takata, N. Happo, H. Ikemoto, T. Shishido, and K. Hayashi, J. Cryst. Growth **311**, 978 (2009).

[8] J. B. Boyce and J. C. Mikkelsen, Jr., J. Cryst. Growth **98**, 37 (1989).

[9] J. Pellicer-Porres, A. Polian, A. Segura, V. Muñoz-Sanjosé, A. Di Cicco, and A. Traverse, J. Appl. Phys. **96**, 1491 (2004).

[10] N. Motta, A. Balzarotti, P. Letardi, A. Kisiel, M. T. Czyżyk, M. Zimnal-Starnawska, and M. Podogòrny, J. Cryst. Growth **72**, 205 (1985).

[11] N. Happo, H. Sato, T. Mihara, K. Mimura, S. Hosokawa, Y. Ueda, and M. Taniguchi, J. Phys.: Condens. Matter **8**, 4315 (1996).

[12] A. Balzarotti, M. Czyżyk, A. Kisiel, N. Motta, M. Podgòrny, and M. Zimnal-Starnawska, Phys. Rev. B **30**, 2295 (1984).

[13] A. Balzarotti, N. Motta, A. Kisiel, M. Zimnal-Starnawska, M. T. Czyżyk, and M. Podgòrny, Phys. Rev. B **31**, 7526 (1985).

[14] J. B. Boyce and J. C. Mikkelsen, Jr., Phys. Rev. B **31**, 6903 (1985).

[15] A. Di Cicco, E. Principi, and A. Filipponi, Phys. Rev. B **65**, 212106 (2002).

[16] L. Vegard, Z. Phys. **5**, 17 (1921).

[17] L. Pauling, *The Nature of the Chemical Bonds* (Cornell University Press, New York, 1967).

[18] M. Tegze and G. Faigel, Nature (London) **380**, 49 (1996).

[19] M. Tegze, G. Faigel, S. Marchesini, M. Belakhovsky, and O. Ulrich, Nature (London) **407**, 38 (2000).

[20] K. Hayashi, in *Advances in Imaging and Electron Physics*, edited by P. W. Hawks (Academic, New York, 2006), Vol. 140, p. 120.

[21] K. Hayashi, Y. Takahashi, E. Matsubara, S. Kishimoto, T. Mori, and M. Tanaka, Nucl. Instrum. Methods Phys. Res. B **196**, 180 (2002).

[22] K. Hayashi, N. Happo, S. Hosokawa, W. Hu, and T. Matsushita, J. Phys.: Condens. Matter **24**, 093201 (2012).

[23] P. M. Len, S. Thevuthasan, C. S. Fadley, A. P. Kaduwela, and M. A. Van Hove, Phys. Rev. B **50**, 11275 (1994).

[24] J. J. Barton, Phys. Rev. Lett. **67**, 3106 (1991).

[25] N. Happo, K. Hayashi, and S. Hosokawa, Jpn. J. Appl. Phys. **49**, 116601 (2010).

[26] *International Tables for Crystallography*, edited by A. J. C. Wilson (Kluwer, Dordrecht, 1992), Vol. C.

[27] C. Kittel, *Introduction to Solid State Physics*, 7th ed. (Wiley, New York, 1996).

[28] S. Sasaki, *KEK Report 90-16* (National Laboratory for High Energy Physics, Tsukuba, Japan, 1990), pp. 1–143.

[29] B. Adams, D. V. Novikov, T. Hiort, G. Materlik, and E. Kossel, Phys. Rev. B **57**, 7526 (1998).

[30] S. Marchesini, N. Mannella, C. S. Fadley, M. A. Van Hove, J. J. Bucher, D. K. Shuh, L. Fabris, M. J. Press, M. W. West, W. C. Stolte, and Z. Hussain, Phys. Rev. B **66**, 094111 (2002).

[31] M. Kopecky, A. Lausi, E. Busetto, J. Kub, and A. Savoia, Phys. Rev. Lett. **89**, 279602 (2002).

[32] P. Korecki, D. V. Novikov, M. Tolkiehn, and G. Materlik, Phys. Rev. B **69**, 184103 (2004).

[33] W. Hu, K. Hayashi, T. Yamamoto, N. Happo, S. Hosokawa, T. Terai, T. Fukuda, T. Kakeshita, H. Xie, T. Xiao, and M. Suzuki, Phys. Rev. B **80**, 060202(R) (2009).

[34] K. Hayashi, T. Hayashi, T. Shishido, E. Matsubara, H. Makino, T. Yao, and T. Matsushita, Phys. Rev. B **76**, 014119 (2007).

[35] M. Tegze, G. Faigel, S. Marchesini, M. Belakhovsky, and A. I. Chumakov, Phys. Rev. Lett. **82**, 4847 (1999).

[36] S. Wei, H. Oyanagi, H. Kawanami, K. Sakamoto, T. Sakamoto, K. Tamura, N. L. Saini, and K. Uosaki, J. Appl. Phys. **82**, 4810 (1997).

[37] K. Hayashi, Y. Takahashi, I. Yonenaga, and E. Matsubara, Mater. Trans. **45**, 1994 (2004).